Poloidal Rotation in TFTR Reversed Shear Plasmas

R. E. Bell,[1] F. M. Levinton,[2] S. H. Batha,[3] E. J. Synakowski,[1] and M. C. Zarnstorff[1]
[1]*Princeton Plasma Physics Laboratory, Princeton, New Jersey 08543*
[2]*Fusion Physics & Technology, Torrance, California 90503*
[3]*Science Research Laboratory, 15 Ward Street, Somerville, Massachusetts 02144*
(Received 27 April 1998)

A bifurcation in the core poloidal rotation of carbon impurity ions in the Tokamak Fusion Test Reactor (TFTR) has been observed prior to the transport bifurcation associated with enhanced reverse shear plasmas. In a narrow radial region of the plasma, the impurity ion poloidal rotation reverses direction. This poloidal flow is associated with the establishment of a large negative radial electric field with strong shear. The measured poloidal velocities before, during, and after this precursor differ from neoclassical predictions. [S0031-9007(98)06912-9]

PACS numbers: 52.55.Fa, 52.25.Fi, 52.30.–q, 52.70.Ds

The understanding of the formation of transport barriers in tokamak plasmas is fundamental to the development of techniques to control such barriers for tailoring profiles and improving operating regimes. A large body of work has been devoted to the study of the edge transport barrier responsible for the improved confinement properties of H-mode plasmas [1,2]. More recently, the study of internal barriers has gained attention, particularly transport barriers formed in enhanced reversed shear (ERS) or negative central shear (NCS) discharges [3,4]. Both H-mode and ERS plasmas exhibit a bifurcation in confinement from the previous plasma state. These confinement improvements result from the establishment of a transport barrier within a few centimeters of the edge for H-mode plasmas and within the inner half radius for ERS plasmas. At the plasma edge, the radial electric field, E_r, and its gradient, E_r', have been linked to the bifurcation dynamics at the H-mode transition. Their role is manifested in a change in the plasma impurity [5] and working ion [6] poloidal flow velocity. The fundamental role of E_r is further evidenced by H-mode-like confinement induced and sustained by the external application of an electric field [7]. For ERS plasmas, E_r and $E \times B$ shear flow are central to the sustainment of high confinement [8].

In this Letter, local poloidal rotation, v_θ, measurements of impurity ions deep in the plasma core are presented for the first time. They reveal that the bifurcation in confinement in ERS plasmas is preceded by a bifurcation in the carbon v_θ. In a narrow radial channel near the radius of the minimum safety factor, $q_{\min}$, the carbon v_θ reverses direction for those discharges which will transit to improved confinement. These v_θ precursors are associated with a large negative E_r, over a few centimeters of radius or a few percent of the minor radius for Tokamak Fusion Test Reactor (TFTR) RS plasmas. The large associated electric field shear determined by these local measurements is easily sufficient to satisfy the rough criterion expressed by Waltz [9] that the shearing rate exceeds the linear growth rate of the fastest growing mode, $\gamma^{\max}$, for turbulence suppression by the decorrelation of the turbulent eddies responsible for radial transport. Also, measurements of the carbon poloidal velocity in the core differ significantly from neoclassical predictions of the carbon poloidal velocity for reverse shear plasmas.

The shearing rate is given by $\omega_{E\times B} = (R^2 B_\theta^2/B)\partial/\partial\psi(E_r/RB_\theta)$, where R is the major radius, B_θ is the poloidal magnetic field, B is the total magnetic field, and ψ is the poloidal magnetic flux [10,11]. This is evaluated using an indirect measurement of E_r obtained from the radial force balance equation, $E_r = \nabla p/(eZn) + v_\phi B_\theta - v_\theta B_\phi$, where p is the ion pressure, e is the electronic charge, Z is the charge number, n is the ion density, v_ϕ is the toroidal velocity, and B_ϕ is the toroidal magnetic field. This equation applies separately to each ion species in the plasma; the pressure and velocity are unique for each species. Carbon p, n, and v_ϕ have been routinely measured on TFTR using charge exchange recombination spectroscopy [12]. The new local measurements of v_θ allow the determination of profiles of E_r and $\omega_{E\times B}$.

Local measurements of v_θ are made by a new spectroscopic diagnostic along with a novel inversion technique [13]. Carbon v_θ profiles were determined by measuring the Doppler shifted emission of the C VI 5291 Å line using charge exchange (CX) emission in the core and intrinsic emission in the outer third of the plasma. The diagnostic incorporated two up-down symmetric sets of sight lines to cancel the effects of the energy dependent CX cross section [14,15] which can seriously distort the measured v_θ profiles. Typically, v_θ measurements in the core using vertical sight lines suffer from radial smearing due to field curvature within the large vertical footprint of the neutral beam. The inversion procedure, using the magnetic geometry, recovers the local v_θ which, in the core, also requires independent knowledge of the neutral beam geometry and a beam attenuation calculation based on separately measured profiles. The temporal resolution

for these measurements was 20 ms with a spatial resolution after inversion of about 3.5 cm.

Deuterium reversed shear discharges were studied at two toroidal magnetic fields, $B_\phi = 4.6$ and 3.4 T. The plasma currents were $I_p = 1.6$ and 1.2 MA, respectively, for the high and low field discharges, resulting in similar edge q values. The plasmas had a major radius of $R = 2.60$ m and a minor radius of $a = 0.95$ m. The reversed magnetic shear was established by early heating with neutral beams during a current ramp. Additional neutral beam heating was then added with sufficient power to produce a transition to enhanced confinement. The neutral beam power was 25–28 MW for high B_ϕ discharges, and 13–15 MW for low B_ϕ. A lithium pellet was injected early in the discharges. Pellet injection seems to provide favorable conditions for a transition, though the mechanism is not understood, and is not always required. In the low field discharges, pellet injection seems to assist in the formation of the negative magnetic shear in the core, as in the pellet enhanced performance regime [16].

Shown in Fig. 1 are parameters from two nearly identical reversed shear discharges. Shortly after the start of the high power heating phase, there is a transport bifurcation which, initially, is chiefly manifested in a change in the rate of rise of the plasma density. Shown in Fig. 1(a) is the local carbon pressure which gives the first indication of a difference between RS and ERS discharges. The difference in carbon pressure between the two discharges is due mostly to the carbon density. Measurements of the carbon poloidal rotation show, in Fig. 1(b), a bifurcation in v_θ about 60 ms prior to the first indication of a transport improvement at a major radius of $R = 3.02$ m which corresponds to $r/a = 0.25$. The direction of rotation of the impurity carbon ions is in the *ion* diamagnetic drift direction, until the bifurcation, when there was a reversal in the direction of rotation of carbon for the discharge that would undergo a transition to ERS. During the ERS phase, the ion thermal confinement in the core was below standard neoclassical values, as previously observed on similar discharges [3].

Some of the low field RS discharges provided the largest observed excursions in v_θ prior to the ERS transition. Figure 2 shows both chord-averaged and inverted profiles of v_θ for a low B_ϕ discharge. The chord-integrated measurements sample emission over an extended radial range outside their tangency radii. The narrow region with flow reversal appears to extend inward in the chord-averaged profile, and becomes more distinct and deeper in the inverted v_θ profile, occupying just one sight line for this discharge. In other discharges, the v_θ excursion often appears simultaneously on two sight lines. The tangency radii of the sight lines are spaced about 3.5 cm apart with a gap in sensitivity of about 1 cm. A positive spike in v_θ appears on the sight line just inside the one with the large negative velocity. This is an artifact of the inversion resulting from a narrow shear layer being misaligned with

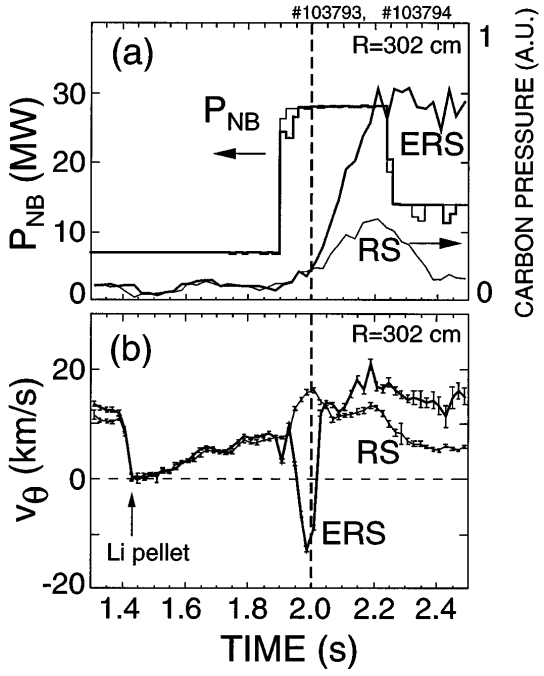

FIG. 1. Comparison of two reverse shear discharges. (a) A transport improvement indicated by the bifurcation in the local carbon pressure at the transition to ERS confinement. (b) A bifurcation in carbon poloidal rotation is observed prior to the transport improvement.

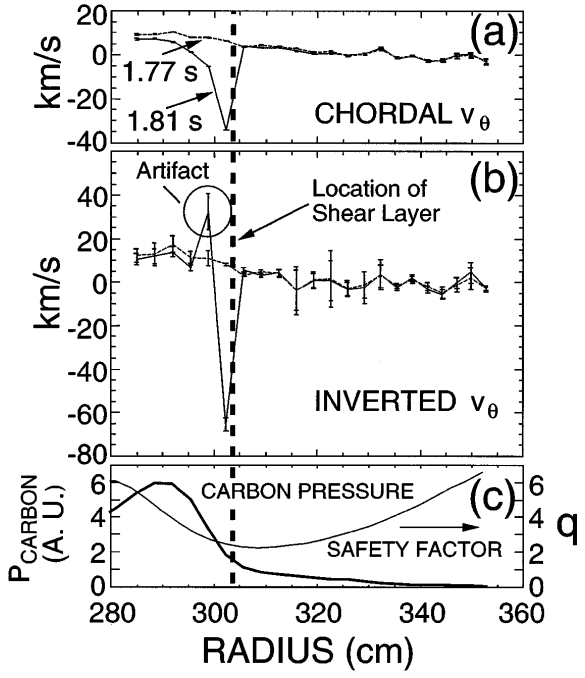

FIG. 2. (a) Chord-averaged carbon v_θ profile for low B_ϕ discharge. (b) Inverted carbon v_θ profile indicates a narrow radial layer with high shear. (c) Location of shear layer is between the high gradient region of carbon pressure and the location of $q_{\min}$.

the sight line locations. A shear layer narrower than the channel-to-channel spacing results in an overshoot of the velocity on the inner adjacent sight line when the layer is not centered. Depending on the location of the reversed flow, the largest v_θ may not be sampled by the nearest sight line. The sight lines inside the shear layer all measure diminishing amounts of the shear layer and thereby provide information on the location of the shear layer, though the width cannot be uniquely determined. The chord-averaged profile can constrain the product of the width of the shear layer, Δr, and the change of the velocity, Δv_θ, where $(\Delta r)(\Delta v_\theta) \approx -220$ cm km/s. From the location of the shear layer and the fact that it is not seen on the next outboard channel, the shear layer is less than 2 cm wide. This implies that $|\Delta v_\theta| > 110$ km/s. Also shown in Fig. 2 is the measured q profile using the motional Stark effect (MSE) diagnostic [17]. The position of the shear layer changed, over one or two sight lines, as discharge parameters varied. The location of the v_θ shear region was always a few centimeters inside the location of $q_{\min}$ for both high and low B_ϕ discharges.

From the radial force balance equation, it is clear that the large excursions in v_θ correspond to a large negative change in E_r. The MSE diagnostic measures the local pitch angle of the magnetic field to determine q, but is also sensitive to E_r in the plasma [18–20]. Large values of E_r contribute to the measured polarization angle of the beam emission used to determine the pitch of the magnetic field. For the low B_ϕ discharges, the magnitude of E_r, its localization, and its transient nature were sufficient to distinguish the contribution of E_r from the magnetic pitch angle contribution to the MSE measurement [20]. In Fig. 3 is a comparison of E_r for the discharge shown in Fig. 2 measured spectroscopically and with the change in E_r from MSE at the nearest radius. There is a good correlation in time and magnitude between the two measurements. This correlation indicates that additional terms in the force balance equation, such as time-dependent terms, are not needed to capture the dynamics of the excursion. Both measurements are observed at one radial location only for this discharge. The MSE channels are spaced about 4 cm apart. The large change in E_r seems to be associated entirely with the poloidal flow with little or no change in the pressure gradient or toroidal flow. The narrowness of the shear layer affects the inferred magnitude of E_r. A shear layer narrower than the 3.5 cm spacing of the poloidal rotation diagnostic implies both a large poloidal flow and a larger E_r. Likewise, the MSE measurement has a radial sensitivity over a 3.5 cm range, such that it measures an average E_r over that region. For a shear layer width of 1 cm, the inferred values of E_r shown in Fig. 3 would triple, thereby increasing the E_r shear by an order of magnitude.

Though the poloidal rotation of the main ions was not measured, something can be said about its behavior during

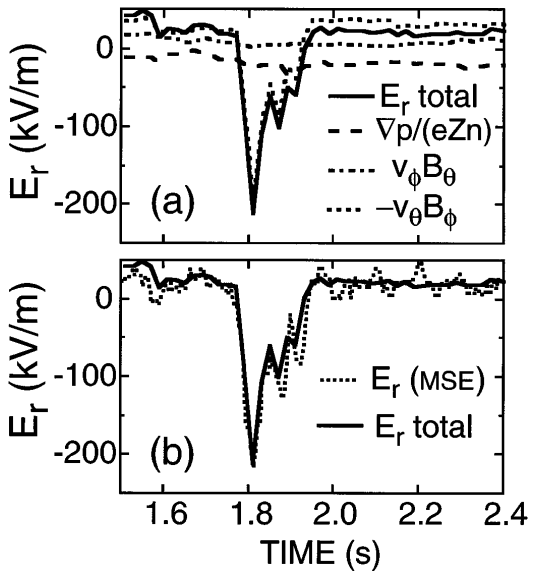

FIG. 3. (a) Total radial electric field during the ERS precursor is determined spectroscopically by summing measured terms from the radial force balance equation. (b) Comparison of E_r determined from MSE and from spectroscopy at the same radial location shows good temporal and quantitative agreement.

the time of the v_θ excursion for carbon. This precursor occurs at a time before there are changes in pressure and temperature associated with enhanced confinement. Although determined from the carbon ions alone, the large E_r is felt by the main ions as well. Since there is little or no change in the pressure profile, as determined by the density and temperature diagnostics, radial force balance indicates that there must also be a strong change in the flow of the main ions. If, like carbon, there is no change in deuterium v_ϕ, then the *change* in the deuterium v_θ would be the same as the *change* in the carbon v_θ with a similar radial extent.

Though the generating mechanism is not yet understood, the large poloidal flows measured for the carbon impurity ions represent large shearing rates, many times larger than necessary to satisfy the nominal criterion of $\omega_{E\times B} \geq \gamma^{\max}$ for an ERS transition. Within the limited data set, however, there was one discharge in which there was no observed poloidal rotation precursor even though a transition to ERS took place, indicating that the conditions for the transition were already marginally present. Every discharge with a poloidal precursor did have a transition. It is therefore likely that these precursors are not necessary for a transition, but do provide an overwhelming push that ensures a transition will take place. The large shear in v_θ and E_r precede the transport improvement and relax as the confinement improvement takes place, indicating that the precursor is associated with triggering the transition only, and not with sustaining the enhanced confinement.

With measurements of v_θ in the plasma core, a comparison can be made to the values calculated using neoclassical theory. Neoclassical calculations were done

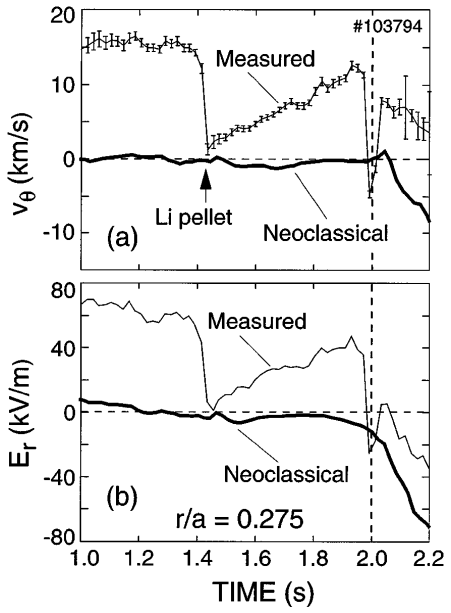

FIG. 4. (a) Measured and neoclassical calculated values of carbon v_θ at $r/a = 0.275$. Vertical dashed line indicates ERS transition time. (b) Measured and neoclassical E_r.

using the treatment of Houlberg *et al.* [21]. In Fig. 4(a) the calculated and measured v_θ are plotted at $r/a = 0.275$ versus time for the high B_ϕ ERS discharge shown in Fig. 1. The neoclassical calculation of v_θ yields a flat profile with little or no poloidal rotation before the transition. The measured v_θ, however, shows a large value early in the discharge which goes to zero at the time of lithium pellet injection. As the plasma recovers from the pellet, the measured v_θ increases with time. Again, an offset between measured and calculated v_θ develops. At the time of the v_θ excursion the measured v_θ dips below the neoclassical v_θ. After the ERS transition, both the measured and neoclassical v_θ become more negative, though an offset between them persists. The reason for this discrepancy between measured and neoclassical values of v_θ is unknown.

The differences between the measured and neoclassical v_θ have an important effect on the inferred E_r and its gradient. Figure 4(b) shows the effect of this difference on E_r. While the neoclassical E_r at $r/a = 0.275$ is nearly zero until the ERS transition, the measured E_r is positive before pellet injection and returns to positive values shortly thereafter, yielding a larger measured E_r' before the transition. Both the neoclassical and measured E_r profiles exhibit a negative well after the transport bifurcation, but the measured well depth is shallower than the neoclassical value, resulting in a smaller measured E_r' after the transition. This would suggest that $\omega_{E\times B}$ was previously underestimated before the transition and overestimated after the transition when neoclassical predictions were used. Previous experiments with RS discharges at lower field [22,23] suggested that $\omega_{E\times B}$ was up to a factor of 3 below $\gamma^{\max}$ at the time of the transition when a neoclassical v_θ was used. These new measurements argue that this may not have been the situation, but that a larger unmeasured shear flow was present.

This work was supported by U.S. Department of Energy Contract No. DE-AC02-76CH03073.

[1] T. N. Carlstrom, Plasma Phys. Controlled Fusion **38**, 1149 (1996), and reference therein.
[2] D. J. Ward, Plasma Phys. Controlled Fusion **38**, 1201 (1996), and reference therein.
[3] F. M. Levinton *et al.*, Phys. Rev. Lett. **75**, 4417 (1995).
[4] E. J. Strait *et al.*, Phys. Rev. Lett. **75**, 4421 (1995).
[5] R. J. Groebner, K. H. Burrell, and R. P. Seraydarian, Phys. Rev. Lett. **64**, 3015 (1990).
[6] J. Kim *et al.*, Phys. Rev. Lett. **72**, 2199 (1994).
[7] R. J. Taylor *et al.*, Phys. Rev. Lett. **63**, 2365 (1989).
[8] E. J. Synakowski *et al.*, Phys. Rev. Lett. **78**, 2972 (1997).
[9] R. E. Waltz, G. D. Kerbel, and J. Milovich, Phys. Plasmas **1**, 2229 (1994).
[10] T. S. Hahm and K. H. Burrell, Plasma Phys. Controlled Fusion **38**, 1427 (1996).
[11] K. H. Burrell, Phys. Plasmas **4**, 1499 (1997).
[12] B. Stratton *et al.*, in *Proceedings of the IAEA Technical Committee Meeting on Time Resolved Two- and Three-Dimensional Plasma Diagnostics, Nagoya, Japan, 1990* (IAEA, Vienna, 1991), p. 78.
[13] R. E. Bell, Rev. Sci. Instrum. **68**, 1273 (1997).
[14] R. B. Howell *et al.*, Rev. Sci. Instrum. **59**, 1521 (1988).
[15] M. von Hellerman *et al.*, Plasma Phys. Controlled Fusion **37**, 71 (1995).
[16] M. Hugon *et al.*, Nucl. Fusion **32**, 33 (1992).
[17] F. M. Levinton *et al.*, Phys. Rev. Lett. **63**, 2060 (1989).
[18] M. C. Zarnstorff, Phys. Plasmas **4**, 1097 (1997).
[19] B. W. Rice, K. H. Burrell, L. L. Lao, and Y. R. Lin-Liu, Phys. Rev. Lett. **79**, 2694 (1997).
[20] F. M. Levinton, R. E. Bell, S. H. Batha, E. J. Synakowski, and M. C. Zarnstorff, Phys. Rev. Lett. **80**, 4887 (1998).
[21] W. A. Houlberg, K. C. Shaing, S. P. Hirshman, and M. C. Zarnstorff, Phys. Plasmas **4**, 3230 (1997).
[22] F. M. Levinton *et al.*, in *Proceedings of the 16th International Conference on Fusion Energy, Montreal, 1996* (IAEA, Vienna, 1997), Vol. 1, p. 211.
[23] E. J. Synakowski *et al.*, Phys. Plasmas **4**, 1736 (1997).